
Article:
Bennett, J, Shrout, T, Zhang, S et al. (5 more authors) (2015) Variation of piezoelectric properties and mechanisms across the relaxor-like/Ferroelectric continuum in BiFeO3-(K0.5Bi0.5)TiO3-PbTiO3 ceramics. IEEE Transactions on Ultrasonics, Ferroelectrics, and Frequency Control, 62 (1). 33 - 45. ISSN 0885-3010

https://doi.org/10.1109/TUFFC.2014.006677

Variation of piezoelectric properties and mechanisms across the relaxor-like/ferroelectric spectrum in $BiFeO_3$-$(K_{0.5}Bi_{0.5})TiO_3$-$PbTiO_3$ ceramics

J.Bennett[1,a)], T. R. Shrout[2], S.J. Zhang[2], H.E. Owston[1], T.J.Stevenson[1], F. Esat[1], A. J. Bell[1] and T. P. Comyn[1]
[1]Institute for Materials Research, School of Process, Environmental and Materials Engineering, University of Leeds, Leeds LS2 9JT, UK.
[2]Materials Research Institute, The Pennsylvania State University, University Park, PA 16802, USA.

Abstract

(1-x-y)$BiFeO_3$-x$(K_{0.5}Bi_{0.5})TiO_3$-$_yPbTiO_3$ piezoelectric ceramics were investigated across the compositional space and contrasted against the $BiFeO_3$-$(K_{0.5}Bi_{0.5})TiO_3$ system, a spectrum of relaxor-like/ferroelectric behavior was observed. Structural and piezoelectric properties were found to be closely related to the $PbTiO_3$ concentration, below a critical concentration, relaxor-type behavior was observed. The mechanisms governing the piezoelectric behavior were investigated with the use of a number of techniques including structural, electrical and imaging techniques. X-ray diffraction established that long-range crystallographic order was promoted above a critical $PbTiO_3$ concentration, $y > 0.1125$. Commensurate with the structural analysis, electric-field induced strain responses showed electrostrictive behavior in the $PbTiO_3$-reduced compositions, with increased piezoelectric switching in $PbTiO_3$-rich compositions. PUND analysis was used to confirm electric-field induced polarization measurements, elucidating that the addition of $PbTiO_3$ increased the switchable polarization and long-range ferroelectric ordering. PFM of the $BiFeO_3$-$(K_{0.5}Bi_{0.5})TiO_3$-$PbTiO_3$ system exhibited typical domain patterns above a critical $PbTiO_3$ threshold, with no ferroelectric domains observed in the lead-free system in the pseudocubic region. Doping of $BiFeO_3$-$PbTiO_3$ has been unsuccessful in the search for high-temperature materials that offer satisfactory piezoelectric properties, however, this system demonstrates that the partial substitution of alternative end-members can be an efficacious method. The partial

substitution of $PbTiO_3$ into $BiFeO_3$-$(K_{0.5}Bi_{0.5})TiO_3$ enables long range crystallographic order, resulting in increased polar order and T_C. The search for novel high-temperature piezoelectric ceramics can therefore exploit the accommodating nature of the perovskite family, which allows significant variance in chemical and physical character in the exploration of new solid-solutions.

Introduction

The ferroelectric and piezoelectric properties of lead zirconate titanate (PZT) have been exploited for both sensing and actuating for over 50 years in applications such as medical ultrasound, sonar systems and diesel fuel injectors [1]. A watershed moment in the advancement of electroceramics was the discovery of $BaTiO_3$ in 1945 which exhibits a perovskite structure that belongs to the general formula ABO_3 and is key to commercial ferroelectric and piezoelectric materials [2]. PZT also belongs to this family, its superior electrical properties are owed to a morphotropic phase boundary (MPB) between the $PbZrO_3$-rich rhombohedral and the $PbTiO_3$-rich tetragonal symmetries [3]. This coupling between the two symmetries allows a significant electromechanical response which manifests as large electric-field induced piezoelectric strains. However, large electric-field induced electrostrictive strains can also be generated by relaxor ferroelectrics although these often suffer from poor temperature stability. PZT exhibits a ferroelectric-paraelectric phase transition temperature, T_C, in the region of 386 °C at which point piezoelectric properties are lost, although practically this temperature is much reduced [4].

A canonical relaxor often cited is $Pb(Mg_{1/3}Nb_{2/3})$ (PMN) [5], the electric-field induced strain response is dominated by the electrostrictive effect and characteristic behavior includes a diffuseness of the temperature dependent properties related to the polarization, such as a

broad maximum in the permittivity accompanied with a shift in the T_C toward higher temperatures and the suppression of permittivity with increasing frequency with no obvious transition at T_{MAX} using x-ray diffraction or optical techniques [6]. The generally recognized origin of this behavior is associated with multiple cations sharing the same lattice-site, leading to a structural instability and frustration of long-range structural ordering. Liu suggested that when multiple ions appear on the same site, local strain fields are created that suppresses long-range strain distortion of the unit cell. This frustrates long-range structure ferroelectric order and manifests as polar nano-regions (PNR). The precise nature of PNRs is still not fully understood due to the difficulty of experimental observation. It is agreed that PNR's are lower-symmetry structural regions embedded in a higher symmetry matrix i.e cubic. A number of systems have demonstrated a compositionally dependent crossover between conventional ferroelectric and relaxor type behaviors such as La-doped PZT, BMT-PZ-PT and PMN-PT [7–9].

Recently, the $xBiFeO_3$-$(1-x)(K_{0.5}Bi_{0.5})TiO_3$ system has been fabricated [10–13], notably exhibiting a 'pseudocubic' region where long-range crystallographic order is frustrated coupled with large electric-field induced strains dominated by the electrostrictive component. A series of publications [13-14] have elucidated the origin of the relaxor-like dielectric properties at high temperature across the compositional space, owed to Maxwell-Wagner relaxation rather than conventional relaxor behavior [16]. A high T_C was identified in the $BiFeO_3$-rich compositions (above 440 ºC where $x > 0.6$), making it a potential candidate as a lead-free high-temperature piezoelectric

An MPB similar to PZT is located between tetragonal and rhombohedral symmetries in the $BiFeO_3$-$PbTiO_3$ system at ~70 mol% $BiFeO_3$, a ferroelectric T_C of 632ºC is reported

for this composition [17-18]. The c/a ratio of the tetragonal phase is ~1.18 at the MPB and this giant tetragonal distortion generates large internal stresses that can inhibit nucleation of new domains and suppress non-180º domain switching [19]. Saturated ferroelectric loops have not thus far been acquired in undoped compositions due to the prohibitively large coercive field, E_C, and DC conductivity at high electric-fields is substantial [20].

In this study, a broad compositional space will be examined with respect to structural and electrical ordering, highlighting the transition from relaxor-like properties at the $BiFeO_3$-$(K_{0.5}Bi_{0.5})TiO_3$ end member to conventional ferroelectric behavior at the $BiFeO_3$-$PbTiO_3$ end member and solid-solutions across the compositional space in between.

Experimental

Ceramic powders of the BF-KBT and BF-KBT-PT ternary system were prepared by conventional solid-state synthesis as previously outlined [12] [21]. Powders were uniaxially pressed at 50 MPa in order to form pellets, followed by cold isostatic pressing at 300 MPa for 10 minutes to increase the green density of the unsintered pellets, these were subsequently sintered between 975ºC-1070ºC and 1035ºC–1065ºC for the $PbTiO_3$-free and $PbTiO_3$-derived compounds respectively. Pellets were then mechanically lapped to <1 mm ensuring that the sample was flat across the entire surface and electroded with a fire-on (550 °C) conductive silver paste (Gwent Group, UK) for electrical measurements.

X-ray diffraction (Phillips X'Pert MPD, Netherlands) was used to identify the crystal structure of each composition. Room temperature X-ray diffraction (XRD) scans in the range $20^o < 2\theta < 60^o$ were measured. This was undertaken on crushed and annealed powders in order to minimize the influence of surface effects such as texture and stress. A 5420 SPM

(Agilent Technologies, USA) was used for PFM imaging. The tip utilized was a NSC14/Ti-Pt probe with a tip radius of ~30 nm with scan times typically consisting of a few minutes.

Room temperature polarization–electric field (PE), strain-electric field (xE) measurements of the BF-KBT compounds were performed with a Radiant ferroelectric tester in conjunction with a non-contact displacement probe (Radiant Technologies, USA). Positive-up–negative-down (PUND) measurements were also performed using a Radiant ferroelectric tester using methods outlined by Dolgos [22]. A pulse and delay of 1 second was used throughout as the parasitic contribution to ferroelectric switching was presumed to be relatively fast i.e. >1 second. In order to record the xE and PE measurements at elevated temperatures a linear variable differential transducer (LVDT) was used in line with a DSP SR830 lock-in amplifier (Stanford Research, USA) and a high voltage TREK 610C power supply (TREK, USA). A National Instruments Data Acquisition Card was used to record the data. Samples were placed in an oil bath with the LVDT fixture suspended in a convection furnace. The temperature was recorded at the sample using a thermocouple and samples were held at the set temperature for 10 minutes before measurements commenced. Relative permittivity was measured over a broad frequency range as a function of temperature using an Agilent 4192A, with a non-inductively wound furnace upon heating using a ramp rate of 3 ºC/min.

The poling conditions (electric field and temperature) were optimized for the various compositions, and varied between 4–8kV/mm and 50–100 ºC. The poling time was held constant at 10 min, after this the samples were removed from the hot oil. The piezoelectric charge coefficient d_{33} was determined with a conventional Berlincourt meter (Piezotest PM300, London, UK).

Results

I. Overview of the Structural and Electrical Properties of the $BiFeO_3$-$(K_{0.5}Bi_{0.5})TiO_3$ Binary System

The $xBiFeO_3$-$(1-x)(K_{0.5}Bi_{0.5})TiO_3$ system has recently been reported by a number of authors across the entire compositional space allowing for a reasonable overview. Based upon the recent reports it is apparent that the structural and electrical properties are heavily dependent upon processing. This section provides the current development and status of the structural and electrical properties of the $BiFeO_3$-$(K_{0.5}Bi_{0.5})TiO_3$ system. A simplified nomenclature will be used interchangeably in this section, for example BF-KBT 4060 relates to x = 0.4.

Upon sintering geometrical density measurements were performed, the theoretical density was calculated by interpolating the densities of the end members, as reported in the literature of 8340 and 6244 kg/m^3 for $BiFeO_3$ [23] and $(K_{0.5}Bi_{0.5})TiO_3$ [24] respectively. It was apparent that with the reduction of $BiFeO_3$ the density decreases significantly although this was found to be in excess of 90% of the theoretical density across the compositional space except at x = 0.1, owed to the reduction of $BiFeO_3$ content and the stabilizing effect that this has upon the $(K_{0.5}Bi_{0.5})TiO_3$ compound, the volatilization of potassium and bismuth is well documented [25]. These density values were similar to those found using standard milling techniques, although Morozov and Matsuo increased the densification (> 95%) with refinement of processing conditions [13], [14].

Laboratory X-ray analysis was used for phase identification on crushed and annealed pellets although the patterns are not presented here, a rudimentary phase diagram is shown in Figure 1 with the T_C measured from permittivity plots as a function of temperature. Single-

phase ceramics belonging to the perovskite structure were produced across the entire compositional space. $BiFeO_3$-rich compositions where x = 0.9 - 0.5 fit that of a rhomobohedrally distorted structure, as typified by splitting of the {111} family of planes. It was noted the $\{113\}_H$, associated with oxygen octahedral tilting, was not observed using conventional XRD. whilst the relative intensity of the (111)/(-111) reflections in the $BiFeO_3$ rich compositions are ca. 1:3, as should be the case for unpoled rhombohedral materials. At x = 0.4, no obvious peak splitting is observed in the {111} or {200} family of planes indicative of a transition to a pseuocubic phase, in contrast to other studies who noted this transition at x = 0.6 [13-14]. It has been suggested that the pseudocubic phase is characterized by nanodomain structures consisting of non-polar cubic and polar rhombohedral structures of the order of 10 nm identified using TEM [11], therefore explaining the absence of rhombohedral or tetragonal splitting using conventional laboratory X-rays. Minor tetragonal peak splitting was observed in the {200} reflection for x = 0.1, characteristic of the transition to the tetragonal phase although these samples were under-sintered (although any increase in sintering temperature resulted in melting of the samples), and may explain the difficulty in observing this transition clearly.

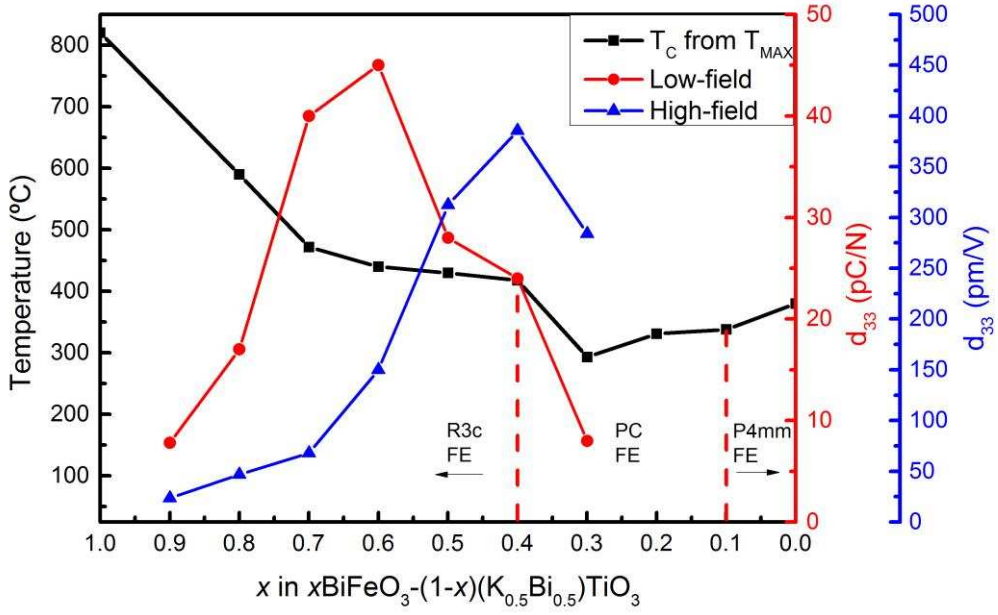

Fig.#1. Phase diagram of the $BiFeO_3$-$(K_{0.5}Bi_{0.5})TiO_3$ system highlighting the low-field, d_{33}, and high-field, d_{33}^*, piezoelectric charge coefficients across the compositional space as well as the Curie temperature

Figure 2(a-b) demonstrates electric-field induced polarization and strain measurements across the compositional space. All measurements were collected at fields of 8.5 kV/mm and at 10 or 0.1 Hz for PE and xE measurements respectively to allow for useful comparison. Well-defined ferroelectric or hysteretic behavior cannot be deduced from these electric-field induced polarization measurements easily, especially at the $BiFeO_3$ rich end of the phase diagram where the materials exhibit behavior consistent with that of a ferroelectric below saturation as observed in PZT. At fields of 13 kV/mm for x = 0.8 the response is an open loop with no hysteresis as these samples are conductive at high fields owed potentially to the multivalent $Fe^{3+/2+}$ cation. The electric-field induced polarization measurement (calculated from an integration of current) becomes problematic when the electrical resistivity is low as conductive "football shaped" loops are often recorded, thus the measurement was performed at slightly higher frequencies (10 Hz) than the xE measurements to negate the effects of electrical conduction which are much reduced as the frequency is increased.

Concave PE loops are exhibited for compositions where x = 0.3-0.6 which is evidence of ferroelectric behavior as endorsed by Scott [26]. PUND measurements also confirmed ferroelectric switching, shown in the next section in Figure 7, as this technique removes the effect of parasitics such as leakage current and polar nano-regions. The polarization values observed here are much lower in the active region (26-28 $\mu C/cm^2$) than those recorded by Matsuo of 52 $\mu C/cm^2$. Whilst the maximum polarization value does not alter significantly

where x = 0.6 - 0.4 the shape of the loop is increasingly linear and slim-loop type behavior was observed. In conventional ferroelectrics, when $T < T_C$, hysteresis loops are square with $P_r \sim P_{SAT}$. The divergence between the P_{SAT} and P_R decreases up to x = 0.6, however, with further addition of $(K_{0.5}Bi_{0.5})TiO_3$ the divergence increases dramatically. These slim loops are often associated with certain classes of relaxor ferroelectrics [6].

An explanation for the relatively low switchable polarization values obtained could be owed to leakage, however, the leakage was not found to be excessive, with values measured found to be typical for $BiFeO_3$-based piezoelectric ceramics. The leakage current density values measured are typically within the same order of magnitude albeit slightly higher than those documented by Matsuo [13], where x = 0.6 and 0.4 at 1 kV/mm J values were between 10^{-7}-10^{-8} A/cm^2, also explained by the different preparation methods utilized.

Electric-field induced strain measurements, shown in Figure 2(b), indicate an increase in the strain response with the addition of $(K_{0.5}Bi_{0.5})TiO_3$, noticeably where x = 0.6 from 0.13% to 0.33% at x = 0.4, the values reported are sizeable although the application of large electric-fields is required, when compared to BFPT system it is apparent that much reduced electric fields are required to cause the onset of strain which is between 7-17 kV/mm in BFPT. Similarly to BFPT the electric-field induced strains observed appear to be largely electrostrictive although this can be owed to different origins, the c/a ratio 1.18 in BFPT and ferroelastic domains are pinned as a result meaning that extraordinarily large fields (up to 20kV/mm) are required to exceed the coercive field and observe the piezoelectric effect in xE measurements, however, the crystallography of the BF-KBT system would suggest that the electrostrictive response is dominant and piezoelectric effect is negligible in the ‘pseudocubic’ region where x <0.4 as little negative strain is observed in general and no

negative strain observed at x = 0.3, a stipulation required for a material to defined as piezoelectric, this response is similar to that displayed by relaxor ferroelectrics.

The electric-field induced strain response is predominantly linear with relatively little hysteretic behavior, which is generally atypical for a piezoelectric material as switching and movement of interfaces such as domain walls occurs when subjected to large electric-fields, especially for non-180 º domains which can be responsible for significant dimensional variations [27]. Morozov also observed this behavior and the proposed origin is due to the presence of polar nano-regions which dominate the electromechanical response as an applied field easily aligns the PNRs but this behavior is not spontaneous i.e. with the absence of an electric-field. Although not presented, the strain response was severely frequency dependent which is common in many lead-free and lead-based relaxor systems.

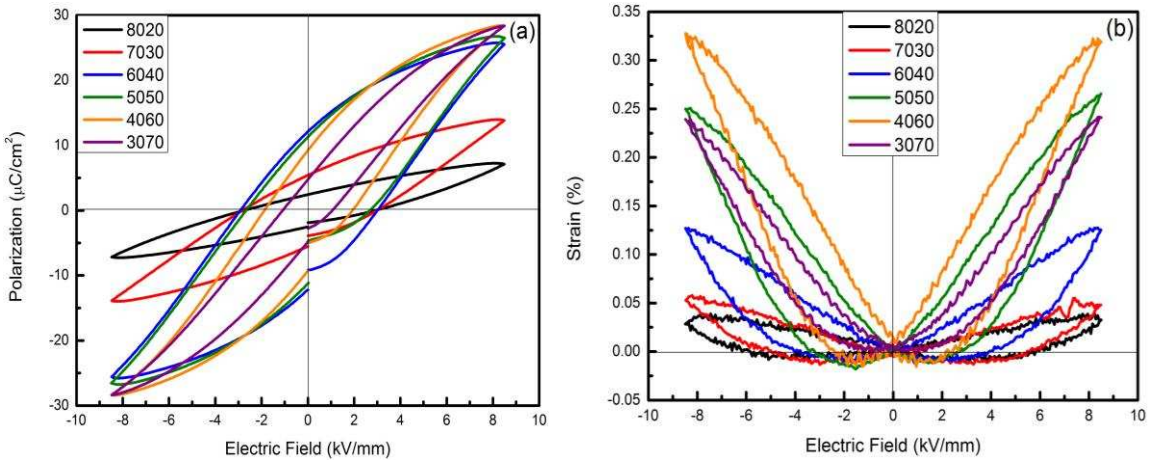

Fig.#2. (a) Bipolar electric-field induced polarization and (b) strain values for $xBiFeO_3$-$(1-x)(K_{0.5}Bi_{0.5})TiO_3$

To showcase the proposed effect of PNRs upon the piezoelectric response the d_{33} is also presented in Figure 1 using two different measurement techniques, one utilising the direct effect with a conventional Berlincourt meter after poling and the other taken from the gradient of the electric-field induced strain values, S_{MAX}/E_{MAX}, which can be seen as the

effective d_{33}^*. Relatively poor, compared to PZT, low-field piezoelectric charge coefficient d_{33} values were recorded across the compositional space with a maximum d_{33} of 45 pC/N observed at x = 0.6, however, the d_{33} values obtained in this study are an order of magnitude greater than in any undoped BFPT composition. N.B. The increase in piezoelectric charge coefficient, d_{33}, for x = 0.6 presented in this contribution compared to an earlier study is due to an optimization of poling conditions. The optimum high-field d_{33}^* value identified was 386 pm/V at x = 0.4, this indicates that the behavior observed in the electric-field induced strain measurements is dominated by electrostriction (PNRs) and the piezoelectric effect is actually limited.

When contrasted to $BiFeO_3$ in a solid-solution with $BaTiO_3$ (c/a >1%) it can be noted that similar behavior was observed with rhombohedrally distorted symmetry at low $BaTiO_3$ concentrations, followed by a broad psuedocubic region consisting of both ferroelectric and non-ferroelectric phases, with tetragonal symmetry noted for $BaTiO_3$ concentrations in excess of 92 mol% [28]. A discrepancy is often observed between the d_{33} and d_{33}^* values, largely due to crystallography and domain structures, however, a disparity of this scale is noteworthy. In the BF-KBT system the location of the peak d_{33} and d_{33}^* values do not correlate, this trend was also identified by Leontsev in the pseudocubic region of the $BiFeO_3$-$BaTiO_3$ system, the origin of the discrepancy was suggested to be due to enhanced domain switching in high-field measurements with poor domain stability leading to reduced low-field coefficients. Future studies of novel piezoelectric ceramics should not solely refer to the d_{33}^* as a means of identifying promising piezoelectric ceramics. As exceptional piezoelectric properties, irrespective of temperature stability, could not be engineered, the use of BF-KBT for sensing and actuating applications was deemed unsuitable.

II. Development of high-temperature $BiFeO_3$-$(K_{0.5}Bi_{0.5})TiO_3$-$PbTiO_3$ piezoelectric ceramics and the relaxor-like/ferroelectric spectrum

X-ray powder diffraction patterns are presented in Figure 3, highlighting a number of compositions that exemplify the transition observed throughout this system. For the composition where x = 0.45 and y = 0.075, a single perovskite phase has formed and sharp peaks recorded with no distinguishable splitting of the reflections. Similar behavior is observed with a reduction of $(K_{0.5}Bi_{0.5})TiO_3$ and increase in $PbTiO_3$ for x = 0.375 and y = 0.1125, although reflections were found to be broader. Profile fitting produced the smallest residuals when fitted to a cubic model. Therefore, the partial substitution of $PbTiO_3$ at these concentrations did not result in the promotion of long-range crystallographic. With further increases in the $PbTiO_3$ concentration obvious peak splitting is still not prevalent although peak-fitting performed using pseudo-Voigt profiles indicated a mixed symmetry region between rhombohedral and tetragonal symmetries. $PbTiO_3$-rich compositions generally belong to the mixed symmetry region, with characteristic peak splitting indicative of a phase co-existence, clearly evidenced from the {200} reflection. As discussed previously, the behavior observed in the $PbTiO_3$-reduced compositions ($y < 0.1125$ $PbTiO_3$) could originate from the existence of PNR's which are difficult to observe due to their relative size. PNRs exist over nanometer-length scales in random directions, as a result the average lattice appears different to the local structure, ergo, the spatial coherence length is not significant enough to observe these features using $CuK\alpha_1$ laboratory x-rays.

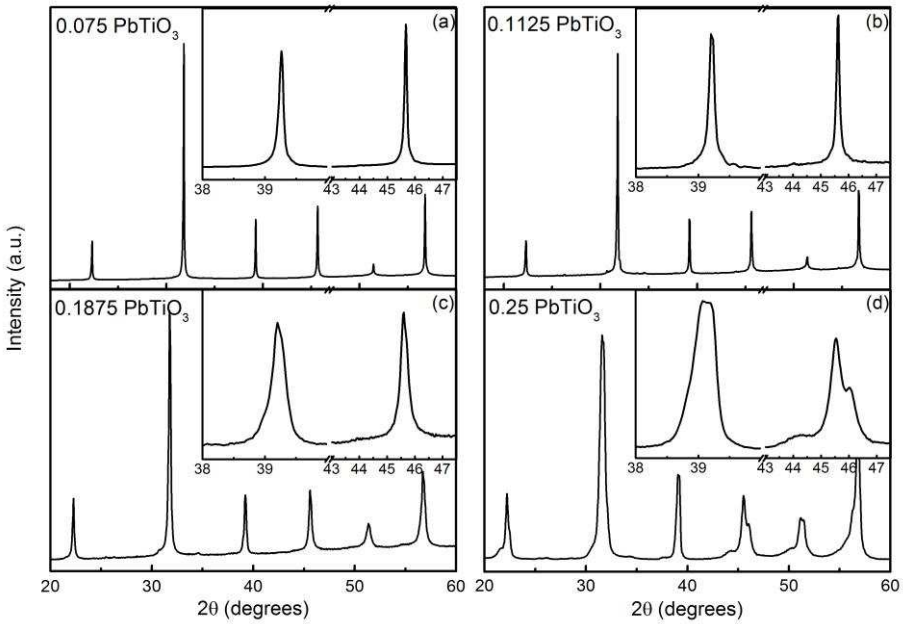

Fig.#3. X-ray diffraction patterns where (a) *x* = 0.45 and *y* = 0.075, (b) *x* = 0.375 and *y* = 0.1125, (c) *x* = 0.225 and *y* = 0.1875 and (d) *x* = 0.15 and *y* = 0.25

Analysis of the {200} family of planes across the compositional space elucidates that the lattice parameters, c/a ratio and tetragonal volume phase fraction all show a strong correlation with the $PbTiO_3$ content not only in the $PbTiO_3$-rich compositions but also toward the $BiFeO_3$-$(K_{0.5}Bi_{0.5})TiO_3$ pseudocubic region, shown in Figure 4. Across the entire system no significant change is observed in the a-lattice parameter, however, the c-lattice parameter changes markedly. Enhanced tetragonality, whereby an increased c/a ratio relative to the $PbTiO_3$ compound is observed with partial substitution of alternative perovskite compounds is incongruous as most Pb or Bi based compounds reduce the tetragonality which subsequently aids in MPB formation [29]. This effect has most notably been observed with the substitution of $BiFeO_3$, although $BiInO_3$, $BiScO_3$, $Bi(Zn_{0.5}Ti_{0.5})O_3$ and $Bi(Zn_{0.75}W_{0.25})$ have resulted in sustained or enhanced tetragonality [29–32]. This behavior is a manifestation of the strong coupling between Pb/Bi and ferroelectrically active displacive B-site cations such as Ti and Fe. The largest tetragonality observed was 1.122 in the composition with y = 0.3375 $PbTiO_3$ which exceeds the $PbTiO_3$ content at the MPB of the BFPT end member,

therefore, the partial substitution of (y = 0.075) $(K_{0.5}Bi_{0.5})TiO_3$ leads to a migration of the MPB. On the contrary, as the $PbTiO_3$ is reduced the c/a ratio decreases, at y < 0.2 $PbTiO_3$ the tetragonality lessens with peak fitting to non-cubic symmetry increasingly difficulty.

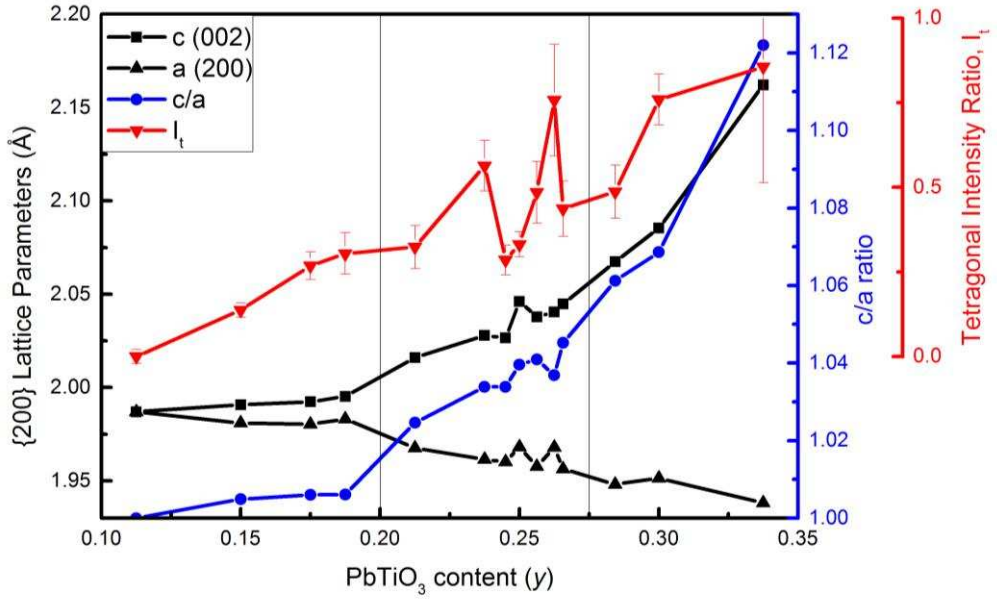

Fig.#4. {200} Lattice Parameters, c/a ratio and tetragonal intensity ratio as a function of $PbTiO_3$ content

Electrical characterization was undertaken on all compositions with a select number presented in Figure 5. These measurements were performed at room temperature and at elevated temperatures to determine the temperature stability of the ferroelectric and piezoelectric response. Samples were measured at 7 kV/mm for ease of comparison, with strain-field loops at 0.1 Hz and polarization-field loops at 3.3 Hz.

Figure 5(a) demonstrates that at room temperature the piezoelectric switching amplitude is small with little negative strain observed, with the response taking a similar shape to that of the lead-free system near to the pseudocubic region. This behavior is to be expected as only small amounts of $PbTiO_3$, y = 0.075, have been partially substituted. At elevated temperatures the loops become much slimmer and the negative strain diminishes,

with the electric-field induced strain response entirely electrostrictive at 150 ºC. Large strains are observed in Figure 5(b), the magnitude of which is greater than for any sample across the $BiFeO_3$-$(K_{0.5}Bi_{0.5})TiO_3$ phase diagram. The origin of the strain response is inferred to be a combination of significant electrostrictive and piezoelectric behaviors at y = 0.1125 $PbTiO_3$. At increased temperatures the negative strain reduces although the total strain increases. The final two compositions, in Figure 5(c) and (d) clearly exhibit piezoelectric switching. The piezoelectric strains observed also increase as a function of temperature due to a 'softening' of the intrinsic and extrinsic contributions to the piezoelectric effect as widely reported in piezoelectric ceramic materials [29-30]. The onset of piezoelectric switching is much reduced compared to $BiFeO_3$-$PbTiO_3$ due to the reduction in the electrical coercive field [20].

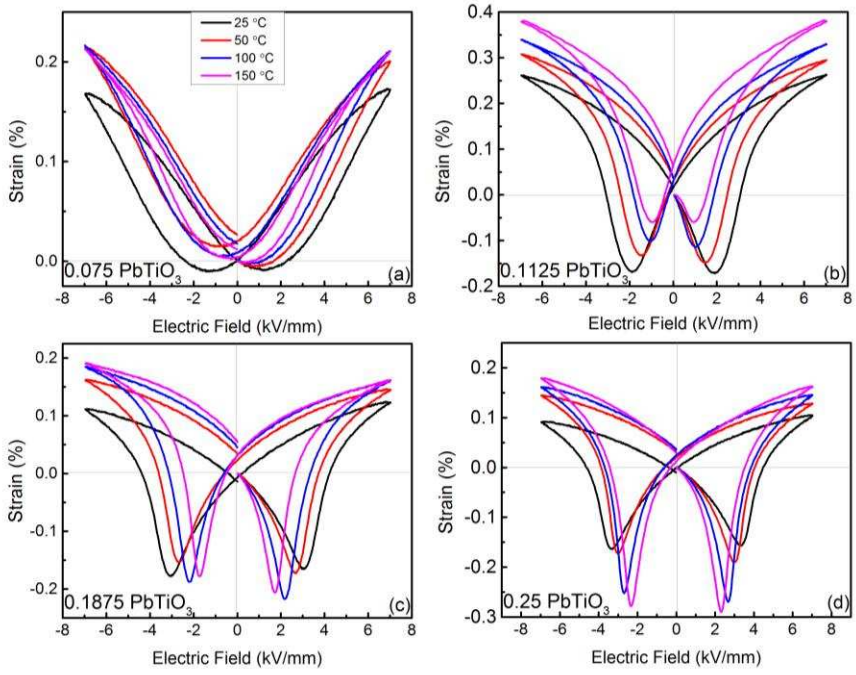

Fig.#5.

Electrical-field induced strain as a function of temperature for selected compositions

Electric-field induced polarization measurements confirm the promotion of long-range polar order with the addition of $PbTiO_3$. Slim loops with a small concave region were observed in Figure 6(a) although evidence for large scale ferroelectric switching is not extensive. An increase in temperature leads to slimming of the PE loops and a small increase in polarization, at 150 ºC conductivity can be seen to contribute. Ferroelectric switching can clearly be distinguished in Figure 6(b) in the xE measurement, this corresponds to the piezoelectric switching identified. The ferroelectric loops remain slim and cannot be described as a classical 'square' hysteresis loops. The measurement at 150 ºC, shown in Figure 6(c), has been omitted due to the high levels of conductivity. Figures(c) and (d) demonstrate behavior consistent with classical ferroelectric materials. The PE loops displayed here are widely representative of the wider compositional space.

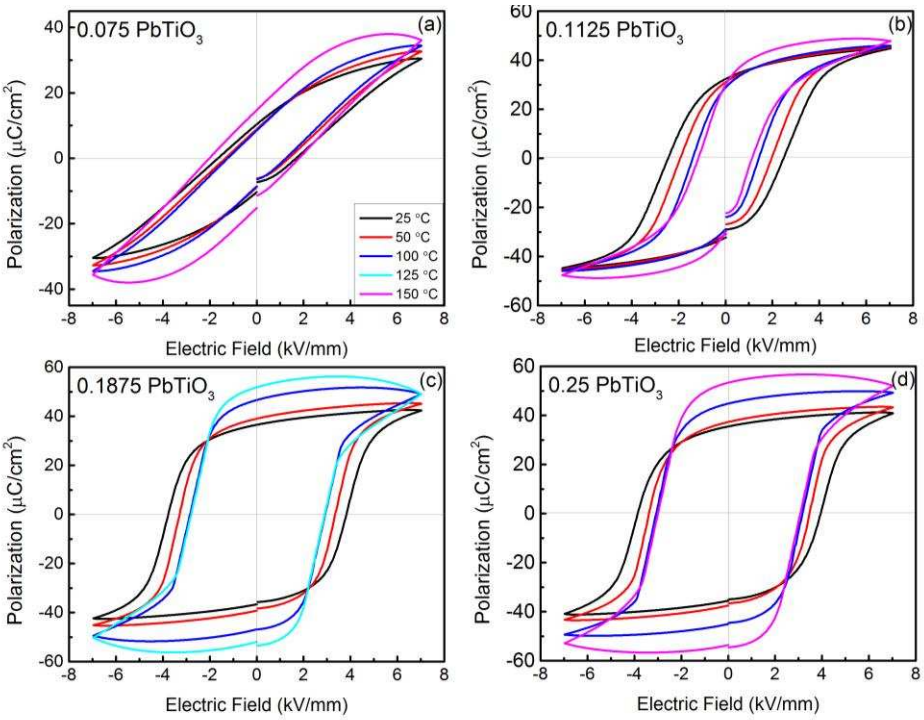

Fig.#6. Temperature dependence of the electrical-field induced polarization for selected compositions

PUND measurements normalized to P_{SAT} are shown in Figure 7. The PUND technique is utilized to separate ferroelectric switching from non-switching parasitics such as leakage current, relaxation processes and polar nano-regions. The value measured is the true ferroelectric switching of the sample as PE loops can often be misrepresentative and PNRs can often mimic ferroelectric behavior. $\Delta P/P_{SAT}$ shows that the lead-free compositions demonstrate limited ferroelectric switching as discussed previously. The compositions shown do not exhibit an obvious electrical coercive field and switching occurs gradually and not at a distinct electric-field especially in the lead-free 4060 BF-KBT composition, this suggests that the coercive field garnered from electric-field induced strain measurements is rather an average from a very broad range of electric-fields. In stark contrast, a large region of the BF-KBT-PT compositional space, even at relatively low $PbTiO_3$ values as shown in the compositions where x = 0.375 0.3, and y = 0.1125 and 0.175 respectively, demonstrated a clearly defined threshold field where ferroelectric switching increases sharply. The magnitude of ferroelectric switching also increases with further partial substitution of $PbTiO_3$ providing substantial evidence of the increase in long-range polar order. For the composition where x = 0.15 and y = 0.3 located near to the BFPT MPB, ferroelectric switching occurs over a broad range of excitation levels, proposed to be due to the large c/a ratio of 1.068 and the significant electrical coercive field of ~6 kV/mm. The ferroelectric switching has not fully saturated which would suggest that with larger electric-fields a greater degree of switching would occur, this is contradictory to other compositions belonging to MSR in the BF-KBT-PT which exhibit behavior consistent with saturation, manifested by flattening of the switchable polarization at a number of different excitation levels.

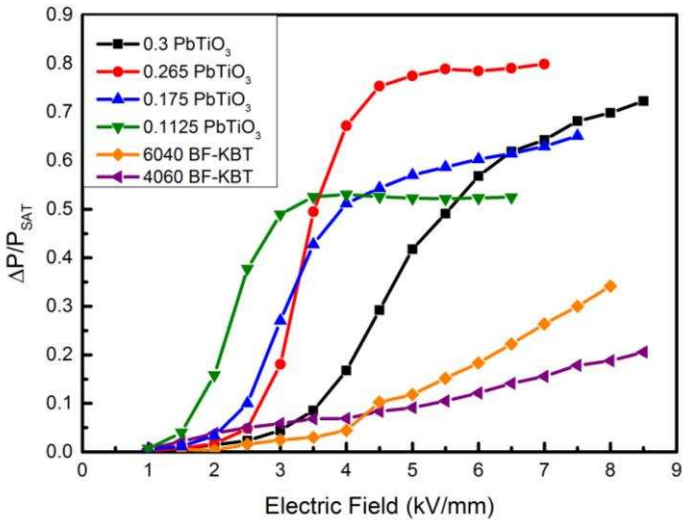

Fig.#7. The switchable polarization normalized to the saturation polarization for compositions with varying $PbTiO_3$ concentrations

A contour plot, shown in Figure 8, has been used to symbolize the piezoelectric charge coefficient d_{33} across the compositional space. Colored markers (black/blue/red/green) mark the compositions fabricated and the order in which each batch was produced, with the black markers produced first and the green markers produced last. The yellow markers situated on the peripheries correspond to values from the literature for the starting end members and $BiFeO_3$-$PbTiO_3$ across the compositional space [3], [31–33], while the values corresponding to the $BiFeO_3$-$(K_{0.5}Bi_{0.5})TiO_3$ system are a result of the authors own work. The darkened blue region symbolizes where the compositional space has not been mapped. As mentioned previously, the most piezoelectrically active composition was found to have a d_{33} of 228 pC/N at room temperature, this value is similar to that of an undoped PZT which demonstrates a d_{33} of 223 pC/N at the MPB [4]. The $PbTiO_3$ concentration is reduced and the $(K_{0.5}Bi_{0.5})TiO_3$ increased through the relaxor-like region the magnitude of the piezoelectric charge coefficients can be seen to reduce significantly.

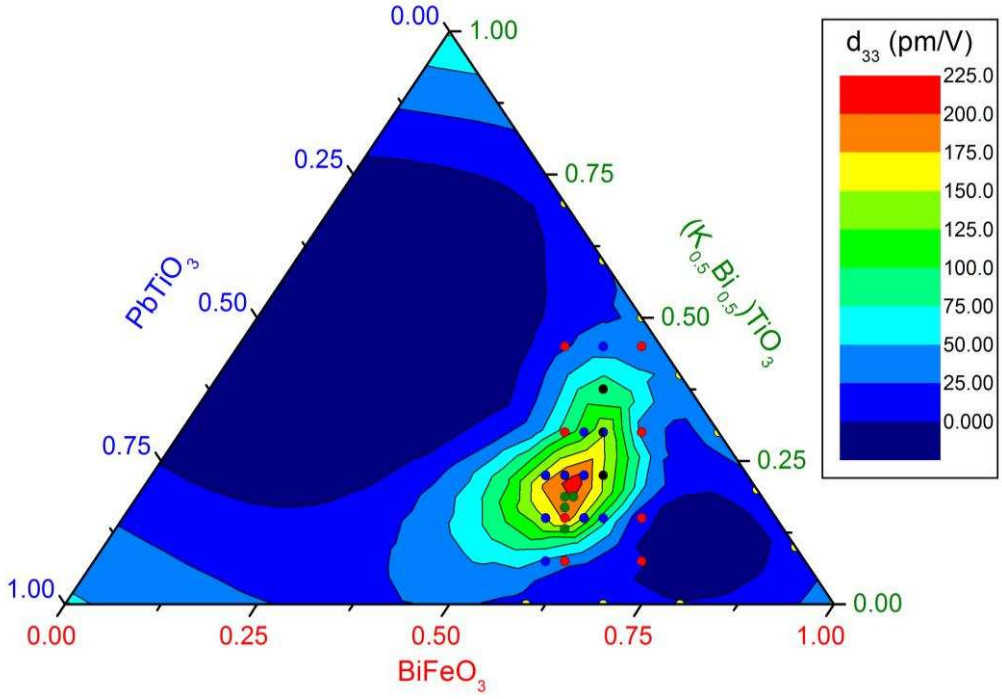

Fig.#8. Contour plot showing the low-signal piezoelectric coefficient d_{33} as a function of composition. Values from the literature have also been included (indicated by the yellow markers) in order to map a greater compositional space

The permittivity as a function of temperature over a range of frequencies (1 kHz-1 MHz) is plotted in Figure 9. The room temperature permittivity values reduced with increasing $PbTiO_3$ and an increase in the T_C was noted across the compositional space. The increase in Curie temperature with increased $PbTiO_3$ may be a result of considerable covalence between the Pb^{2+} and Ti^{4+} cations, coupled with the reduction in $(K_{0.5}Bi_{0.5})TiO_3$ which has a modest T_C and also exhibits a transition to a pseudocubic structure at 270ºC before the T_C at 380ºC [38]. The dielectric loss was enhanced for $PbTiO_3$-rich compositions and this increased sharply as a function of temperature, highlighting the problems facing $BiFeO_3$-derived compounds, that potentially inhibit their use in high-temperature devices.

Commensurate with decreasing $PbTiO_3$, significant peak broadening of the permittivity peaks with increasing frequency occurred. This was accompanied with a shift in the T_C toward higher temperatures and the suppression of permittivity with increasing frequency, further evidence of relaxor-like behavior. Proposed to be a consequence of A-site disorder as the difference in ionic radii between K^+, Pb^{2+} and Bi^{3+} of 1.64, 1.49 and 1.36 Å respectively is considerable. The various frequencies do not converge above the T_{max} in compositions with reduced $(K_{0.5}Bi_{0.5})TiO_3$ due to conductivity, especially prevalent at lower frequencies.

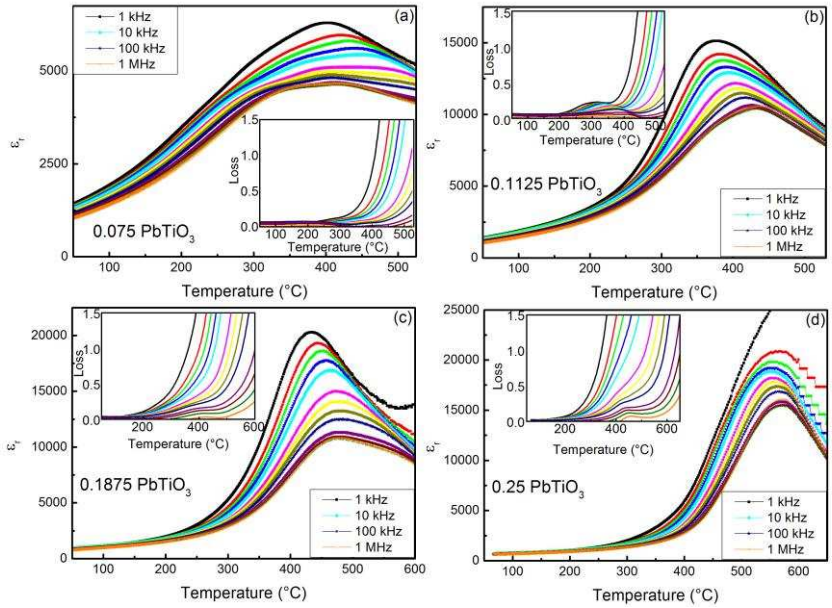

Fig.#9. Permittivity as function of temperature. The insets show the loss as a function of temperature for each composition

Figure 10 shows PFM images on polished surfaces of BF-KBT and BF-KBT-PT with the sample topography presented on the left and the out-of-plane piezoresponse on the right. The first images belong to the pseudocubic region in the 4060 BF-KBT composition which also exhibited the largest electric-field induced strain values although reduced piezoelectric coefficients compared to the 6040 BF-KBT composition. The out-of-plane response, Figure 10(b), confirms a barren piezoelectric response with no evidence of ferroelectric domains on the scales examined. The 6040 BF-KBT piezoresponse, highlighted in Figure 10(d), is shown

not to correlate with the topographical image thus confirming the topography signal is independent to the out-of-plane response associated with piezoelectric ordering. The domains shown are similar to fractal domains that have been widely observed in $BiFeO_3$-derived ultrathin films, these are typically much smaller in size although similar in morphology [39]. However, the electrostrictive effect in this composition was largely dominant and this behavior has to some extent been confirmed by the PFM responses as some piezoelectric responses have been observed in these isolated piezoelectric 'islands'. It is possible that piezoelectric regions could exist within a matrix that behaves as an electrostrictor, similar to some relaxor systems that are thought to contain PNR's in a cubic matrix, elemental segregation has not been excluded as a possible explanation although it is not thought to be probable.

The next series of images are of the BF-KBT-PT system, shown in Figures(e-f), whereby the $PbTiO_3$ content is much reduced although a relatively large room temperature d_{33} was still measured in this composition (using a berlincourt meter of 180 pC/N), however, pseudocubic peaks (that can be fitted to mixed symmetry rhombohedral and tetragonal phases with the lowest residual) are elucidated with the use of XRD. The topography demonstrates some scratching although these can clearly be identified, as the striations are linear. Here, the domains can be characterized as "labyrinthe"-type domains [8], which have been observed in both lead-free and lead-based relaxor ferroelectrics whereby polar regions with a seemingly random trace similar to watermarks are observed. These are suggested to also correspond to 180º domain walls, those observed here are much larger than those observed in $Pb_{0.9125}La_{0.0975}(Zr_{0.65}Ti_{0.35})_{0.976}O_3$ (PLZT) [8] which are ~50 nm in size but similar to those observed in $0.9Pb(Mg_{1/3}Nb_{2/3})O_3$-$0.1PbTiO_3$ [40]. The domains observed in this system are ~200-500 nm in size and much larger than the hypothesized polar nano-regions. Kalinin

suggested that domains of this type are due to the presence of static PNR's, they are defined as static as the imaging timescale, typically a few minutes, allows for their observation.

The $PbTiO_3$-rich composition is presented in Figure 10(g-h), typical domain structures are observed, an obvious piezoelectric response can be confirmed. Domain patterns show no correlation with topography. The piezoresponse within the grain itself demonstrates both 180º domains and 90º domains although these are much less obvious. The polarization vector of the 180º domains in the vertical phase figure displays alignment of the c-axis in both up and down directions. A watermark can be observed in the bottom right-hand side of the grain and the polarization vector can be seen to switch that is commensurate with 180º domain walls.

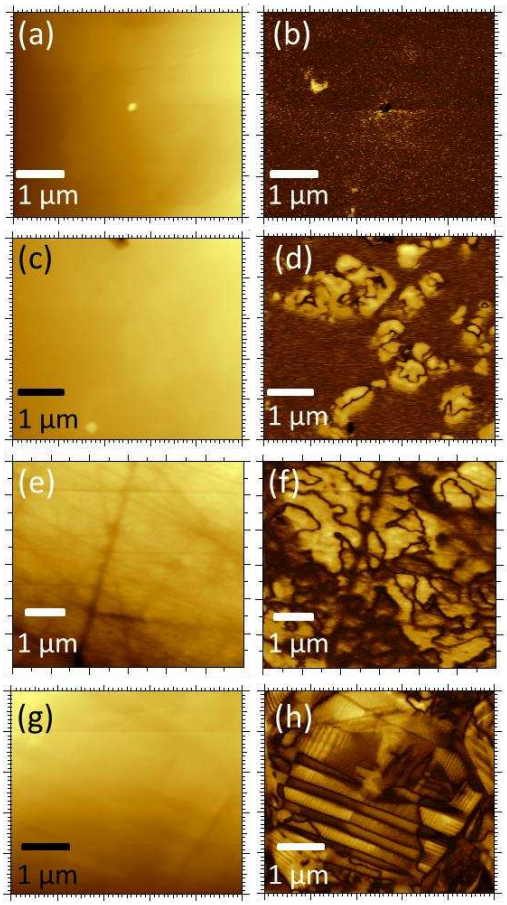

Fig.#10. PFM images of polished samples showing the topography (left) and out-of-plane PFM response (right) for (a-b) 4060 BF-KBT (c-d) 6040 BF-KBT (e-f) $PbTiO_3$-reduced BF-KBT-PT and (g-h) $PbTiO_3$-rich BF-KBT-PT samples.

This technique does not prove evidence for the existence of polar nano-regions which are anticipated to be a handful of unit cells in size, however, long-range ferroelectric order manifested in the piezoresponse can be ruled out. If the PNRs were spatially ordered then it is anticipated that XRD would allow detection due to the cumulative effect of these regions. This technique does not rule out the possibility of these PNRs being temporally ordered. Due to the limitations of the temporal resolution of the equipment, which scans over the course of minutes, it would not be possible to observe PNRs. It does confirm ferroelectric switching in the lead-based compositions across a broad compositional space while the origin of the behavior in the lead-free system is hitherto unconfirmed.

Conclusions

$BiFeO_3$-$(K_{0.5}Bi_{0.5})TiO_3$ ceramics were fabricated across the compositional space revealing rhombohedral symmetry in the $BiFeO_3$-rich compositions, tetragonal symmetry in the $(K_{0.5}Bi_{0.5})TiO_3$-rich compositions and a broad pseudocubic region between the two end members in which relaxor-like ferroelectric properties were dominant. Electric-field induced strains were substantial in this pseudocubic region although negative switching was minimal and low-field piezoelectric charge coefficients, d_{33}, were almost an order of magnitude lower than the corresponding high-field, d_{33}^*, values. This disparity proposed to be a result of the existence of polar nano-regions affecting domain stability upon removal of an applied electric-field.

Consequently, the partial substitution of $PbTiO_3$ into the $BiFeO_3$-$(K_{0.5}Bi_{0.5})TiO_3$ system was utilized in order to promote long-range structural and polar order. Structural analysis across the compositional space elucidates that the lattice parameters, c/a ratio and tetragonal volume phase fraction all show a strong correlation with the $PbTiO_3$ concentration,

below y = 0.2 $PbTiO_3$ the tetragonality lessens markedly. An increase in $PbTiO_3$ also resulted in a gradual increase in electric-field induced strains due to piezoelectric switching rather than the electrostrictive effect. The piezoelectric strains observed also increased as a function of temperature due to a 'softening' of the intrinsic and extrinsic contributions to the piezoelectric effect. Electric-field induced polarization and PUND measurements confirm that long-range polar order is promoted with the addition of $PbTiO_3$. Dielectric measurements revealed a transition from relaxor-like behavior to conventional ferroelectric behavior albeit with high conductivity leading to a lack of convergence at high temperatures for low frequency permittivity plots. PFM measurements displayed a lack of ferroelectric domains in the pseudocubic region of the lead-free system while the composition that displayed the largest piezoelectric charge coefficients displayed a largely electrostrictive matrix with isolated piezoelectric 'islands'. In $PbTiO_3$-reduced compositions in the BF-KBT-PT system "labyrinthe"-type domains consistent with relaxor ferroelectric behavior was observed while $PbTiO_3$-rich composition displayed conventional ferroelectric order. $PbTiO_3$ therefore enables long-range crystallographic order, manifested in greater polar order and T_C.

Acknowledgements

We are grateful to the EPSRC for funding this project (EP/P505593/1), and the World Universities Network for providing financial assistance.

References

[1] B. Jaffe, R. S. Roth, and S. Marzullo, "Piezoelectric Properties of Lead Zirconate-Lead Titanate Solid-Solution Ceramics," J. Appl. Phys., vol. 25, no. 6, pp. 809–810, 1954.

[2] G. H. Haertling, "Ferroelectric Ceramics: History and Technology," J. Am. Ceram. Soc., vol. 82, no. 4, pp. 797–818, 1999.

[3] B. Jaffe and W. R. Cook, Piezoelectric Ceramics, no. 3. London: Academic Press, 1971.

[4] D. A. Berlincourt, C. Cmolik, and H. Jaffe, “Piezoelectric Properties of Polycrystalline Lead Titanate Zirconate Compositions,” Proc. IRE, vol. 48, no. 2, pp. 220–229, 1960.

[5] A. A. Bokov and Z. G. Ye, “Recent progress in relaxor ferroelectrics with perovskite structure,” J. Mater. Sci., vol. 41, no. 1, pp. 31–52, 2006.

[6] L. E. Cross, “Relaxor ferroelectrics,” Ferroelectrics, vol. 76, no. 1, pp. 241–267, 1987.

[7] G. A. Samara and E. L. Venturini, “Ferroelectric/relaxor crossover in compositionally disordered perovskites,” Phase transitions, vol. 79, no. 1–2, pp. 21–40, 2006.

[8] V. V Shvartsman, A. L. Kholkin, A. Orlova, D. Kiselev, A. A. Bogomolov, and A. Sternberg, “Polar nanodomains and local ferroelectric phenomena in relaxor lead lanthanum zirconate titanate ceramics,” Appl. Phys. Lett., vol. 86, no. 20, p. 094102, 2005.

[9] A. I. Frenkel, D. M. Pease, J. Giniewicz, E. A. Stern, D. L. Brewe, M. Daniel, and J. Budnick, “Concentration-dependent short-range order in the relaxor ferroelectric (1−x)Pb(Sc,Ta)O3-xPbTiO3,” Phys.l Rev. B, vol. 70, no. 1, p. 14106, 2004.

[10] J. M. Kim, Y. S. Sung, J. H. Cho, T. K. Song, M. H. Kim, H. H. Chong, T. G. Park, D. Do, and S. S. Kim, “Piezoelectric and Dielectric Properties of Lead-Free (1- x)(Bi 0.5 K 0.5)TiO 3 - x BiFeO 3 Ceramics,” Ferroelectrics, vol. 404, no. 1, pp. 88–92, Oct. 2010.

[11] T. Ozaki, H. Matsuo, Y. Noguchi, M. Miyayama, and S. Mori, “Microstructures Related to Ferroelectric Properties in (Bi0.5K0.5)TiO3–BiFeO3,” Jpn. J. Appl. Phys., vol. 49, no. 9, 2010.

[12] J. Bennett, A. J. Bell, T. J. Stevenson, R. I. Smith, I. Sterianou, I. M. Reaney, and T. P. Comyn, “Multiferroic properties of BiFeO3-(K0.5Bi0.5)TiO3 ceramics,” Mater. Lett., vol. 94, no. 0, pp. 172–175, 2013.

[13] H. Matsuo, Y. Noguchi, M. Miyayama, M. Suzuki, A. Watanabe, S. Sasabe, T. Ozaki, S. Mori, S. Torii, and T. Kamiyama, “Structural and piezoelectric properties of high-density (Bi0.5K0.5)TiO3-BiFeO3 ceramics,” J. Appl. Phys., vol. 108, no. 10, pp. 104103–104106, 2010.

[14] M. I. Morozov, M. A. Einarsrud, and T. Grande, “Polarization and strain response in (Bi0.5K0.5)TiO3-BiFeO3 ceramics,” Appl. Phys. Lett., vol. 101, no. 25, p. 252904, 2012.

[15] M. I. Morozov, M. A. Einarsrud, T. Grande, and D. Damjanovic, “Lead-Free Relaxor-Like 0.75Bi0.5K0.5TiO3-0.25BiFeO3 Ceramics with Large Electric Field-Induced Strain,” Ferroelectrics, vol. 439, no. 1, pp. 88–94, 2012.

[16] M. I. Morozov, M.-A. Einarsrud, and T. Grande, “Control of conductivity and electric field induced strain in bulk Bi0.5K0.5TiO3–BiFeO3 ceramics,” Appl. Phys. Lett., vol. 104, no. 12, p. 122905, 2014.

[17] Y. N. Venevstev, “No Title,” Sov. Phys. Crystallogr., vol. 5, no. 594, 1960.

[18] V. V. S. S. Sai Sunder, A. Halliyal, and A. M. Umarji, “Investigation of tetragonal distortion in the (PbTiO3)-(BiFeO3) system by high-temperature x-ray diffraction,” J. Mater. Res., vol. 10, pp. 1301–1306, 1995.

[19] T. Leist, T. Granzow, W. Jo, and J. Rodel, “Effect of tetragonal distortion on ferroelectric domain switching: A case study on La-doped BiFeO3-PbTiO3 ceramics,” J. Appl. Phys., vol. 108, no. 1, pp. 14103–14106, 2010.

[20] T. P. Comyn, T. Stevenson, and A. J. Bell, “Piezoelectric properties of BiFeO 3 – PbTiO 3 ceramics,” J. Phys. IV Proc., vol. 128, no. c, pp. 13–17, 2005.

[21] J. Bennett, A. J. Bell, T. J. Stevenson, and T. P. Comyn, “Tailoring the structure and piezoelectric properties of BiFeO3-(K0.5Bi0.5)TiO3–PbTiO3 ceramics for high temperature applications,” Appl. Phys. Lett., vol. 103, no. 15, p. -, 2013.

[22] M. Dolgos, U. Adem, X. Wan, Z. Xu, A. J. Bell, T. P. Comyn, T. Stevenson, J. Bennett, J. B. Claridge, and M. J. Rosseinsky, “Chemical control of octahedral tilting and off-axis A cation displacement allows ferroelectric switching in a bismuth-based perovskite,” Chem. Sci., no. 3, pp. 1426–1435, 2012.

[23] S. M. Selbach, M.-A. Einarsrud, T. Tybell, and T. Grande, “Synthesis of BiFeO3 by Wet Chemical Methods,” J. Am. Ceram. Soc., vol. 90, no. 11, pp. 3430–3434, 2007.

[24] P. V. B. Rao, E. V Ramana, and T. B. Sankaram, “Electrical properties of (K0.5Bi0.5)TiO3,” J. Alloys Compd., vol. 467, no. 1–2, pp. 293–298, 2009.

[25] O. N. Razumovskaya, T. B. Kuleshova, and L. M. Rudkovskaya, “Formation Reactions of BiFeO3, (K0.5Bi0.5)TiO3 and (Na0.5Bi0.5)TiO3,” Inorg. Mater., vol. 19, no. 1, pp. 96–99, 1983.

[26] J. F. Scott, “Ferroelectrics go bananas,” J. Phys. Condens. Matter, vol. 20, no. 2, p. 21001, 2008.

[27] T. Rojac, M. Kosec, and D. Damjanovic, “Large Electric-Field Induced Strain in BiFeO3 Ceramics,” J. Am. Ceram. Soc., vol. 94, no. 12, pp. 4108–4111, 2011.

[28] S. O. Leontsev and R. E. Eitel, “Origin and magnitude of the large piezoelectric response in the lead-free (1–x)BiFeO3–xBaTiO3 solid solution,” J. Mater. Res., vol. 26, no. 01, pp. 9–17, 2011.

[29] D. M. Stein, M. R. Suchomel, and P. K. Davies, “Enhanced tetragonality in (x)PbTiO3-(1 - x)Bi(B’B")O3 systems: Bi(Zn3/4W1/4)O3,” Appl. Phys. Lett., vol. 89, no. 13, pp. 132903–132907, 2006.

[30] S. Zhang, R. Xia, C. A. Randall, T. R. Shrout, R. Duan, and R. F. Speyer, “Dielectric and piezoelectric properties of niobium-modified BiInO3-PbTiO3 perovskite ceramics with high Curie temperatures,” J. Mater. Res., vol. 20, no. 8, pp. 2067–2071, 2005.

[31] R. E. Eitel, C. A. Randall, T. R. Shrout, and S. E. Park, “Preparation and characterization of high temperature perovskite ferroelectrics in the solid-solution (1-x)BiScO3-xPbTiO3,” Jpn. J. Appl. Phys., vol. 41, no. 4A, pp. 2099–2104, 2002.

[32] M. R. Suchomel and P. K. Davies, “Enhanced tetragonality in (x)PbTiO3-(1− x)Bi(Zn0.5Ti0.5)O3 and related solid solution systems,” Appl. Phys. Lett., vol. 86, p. 262905, 2005.

[33] T. Sebastian, I. Sterianou, D. Sinclair, A. J. Bell, D. A. Hall, and I. Reaney, “High temperature piezoelectric ceramics in the Bi(Mg1/2Ti1/2)O3-BiFeO3-BiScO3-PbTiO3 system,” J. Electroceramics, vol. 25, no. 2, pp. 130–134, 2010.

[34] J. Chen, X. Tan, W. Jo, and J. Rödel, “Temperature dependence of piezoelectric properties of high-TCBi(Mg1/2Ti1/2)O3–PbTiO3,” J. Appl. Phys., vol. 106, no. 3, p. 034109, 2009.

[35] Y. Hiruma, R. Aoyagi, H. Nagata, and T. Takenaka, “Ferroelectric and Piezoelectric Properties of (Bi 1/2 K 1/2)TiO 3 Ceramics,” Jpn. J. Appl. Phys., vol. 44, no. 7R, p. 5040, 2005.

[36] T. Rojac, B. Budic, N. Setter, and D. Damjanovic, “Strong ferroelectric domain-wall pinning in BiFeO3 ceramics,” J. Appl. Phys., vol. 108, no. 7, pp. 74107–74108, 2010.

[37] T. P. Comyn, T. Stevenson, and A. J. Bell, “Piezoelectric properties of $BiFeO_3$-$PbTiO_3$ ceramics,” Applications of Ferroelectrics, 2004. ISAF-04. 2004 14th IEEE International Symposium on. pp. 122–125, 2004.

[38] V. V Ivanova, A. G. Kapyshev, Y. N. Venevtsev, and G. S. Zhdanov, “X-ray determination of the symmetry of elementary cells of the ferroelectric materials (K0. 5Bi0. 5) TiO3 and (Na0. 5Bi0. 5) TiO3 and of high-temperature phase transitions in (K0. 5Bi0. 5) TiO3,” Izv. Akad. Nauk SSSR, vol. 26, pp. 354–356, 1962.

[39] R. Ranjith, R. V. K. Mangalam, P. Boullay, A. David, M. B. Lepetit, U. Lüders, W. Prellier, A. Da Costa, A. Ferri, R. Desfeux, G. Vincze, Z. Radi, and C. Aruta, “Constrained ferroelectric domain orientation in (BiFeO3)m(SrTiO3)n superlattice,” Appl. Phys. Lett., vol. 96, no. 2, p. 022902, 2010.

[40] A. A. Bokov, B. J. Rodriguez, X. Zhao, J.-H. Ko, S. Jesse, X. Long, W. Qu, T. H. Kim, J. D. Budai, and A. N. Morozovska, “Compositional disorder, polar nanoregions and dipole dynamics in Pb (Mg1/3Nb2/3) O3-based relaxor ferroelectrics,” Zeitschrift für Krist. Cryst. Mater., vol. 226, no. 2, pp. 99–107, 2011.